

Double diffusive convection (DDC) of micropolar nanofluids fluid in a permeable medium

Prof.Mahabaleshwara K.N

Asst Professor

Dept of Mathematics

Smt.Indira Gandhi Govt First Grade Womens's College

Sagar

Abstract:

In this paper we present a nonlinear security examination of the beginning of twofold diffusive convection of a scantily pressed micropolar liquid in a permeable medium layer immersed by a nanofluid. Our nonlinear investigation gives not just the beginning limit of limited adequacy movement yet in addition data about warmth and mass vehicle as far as the warm Nusselt number, the nanoparticle focus Nusselt number, and the solute fixation Nusselt number. The basic Rayleigh number and the wave number for the stationary and the oscillatory modes are acquired logically. The impacts of different parameters on the stationary and oscillatory convection are appeared. The reliance of the stationary or the oscillatory convection on the permeable parameter and the parameters engaged with micropolar liquids is likewise examined. Besides, we examine the impacts of time on the transient Nusselt number and the Sherwood number. These numbers are observed to be oscillatory for little estimations of t . In any case, for enormous t , both the transient Nusselt number and the Sherwood number methodology their enduring state esteems.

Keywords: Rayleigh-Benard convection, nanofluid, micropolar fluid.

1. Introduction

Lately, an investigation of micropolar liquid conduct has been an intriguing region of research. Since the micropolar liquid comprises of haphazardly situated atoms and since every volume component of the liquid has interpretation just as turn movements, the examination of physical issues with these liquids has uncovered a few fascinating marvels not found with Newtonian liquids. The micropolar liquids are liquids with microstructure and have a place with a class of liquids with nonsymmetrical stress tensor alluded to as polar liquids. Physically, they speak to liquids comprising of arbitrarily arranged particles suspended in a gooey medium (Lukaszewicz, [1]), and they are essential to designers and researchers. The definition of a general hypothesis of micropolar liquids was given by Eringen [2]. In this hypothesis, the continuum is viewed as a lot of organized particles which have mass and speed, yet additionally a substructure. That is, every material volume component contains microvolume components that can decipher and turn autonomously of the movement of macrovolume. In this model, two free kinematic vector fields are presented: One speaking to the interpretation speeds of the liquid particles, and the other, called the microrotation vector, speaking to rakish (turn) speeds of the particles. (See [3] for subtleties.) This hypothesis has opened up new thoughts in the material science of liquid stream and warmth move.

Since the nanoparticles are materials of nanometer size having special physical and concoction properties, they have mechanical applications. Nanofluids are strong fluid composite materials comprising of

strong nanoparticles or nanofibers with sizes commonly of 1-100 nm suspended in fluid. An examination with nanofluid has pulled in light of a legitimate concern for analysts as of late because of warm upgrade properties. Be that as it may, issues of rheology and strength are intensified at high focuses, blocking the across the board utilization of regular slurries as warmth move liquids.

During the most recent quite a few years, the investigation of liquid stream and warmth move in permeable media has gotten extensive premium. This is principally a result of the various utilizations of course through permeable media, for example, transport forms in aquifers, geothermal extraction, stockpiling of radioactive atomic waste, partition forms in concoction ventures, filtration, groundwater contamination, transpiration cooling, fiber protection, and so on.

The issue of twofold diffusive convection in permeable media has pulled in significant intrigue in view of its wide scope of utilizations, from the cementing of paired blends to the movement of solutes in water-soaked soils. Geophysical frameworks, movement of dampness through air contained in stringy protection, and electro-science are a portion of different models.

At the point when two diffusive properties are available in a framework, at that point the insecurities can happen just in the event that one of the parts is destabilizing. Whenever warmth and mass exchange happen all the while in a moving liquid, the connection between the transitions and the driving possibilities are of progressively unpredictable in nature. It has been discovered that a vitality transition can be produced by temperature slope as well as by sythesis angles. The vitality transition brought about by a sythesis inclination is known as the Dufour or dispersion thermo impact. Then again, the mass transitions can likewise be made by temperature angles, and this is the Soret or warm dispersion impact. On the off chance that the cross-dissemination terms are incorporated into the species transport conditions, at that point the circumstance will be very extraordinary. Because of the cross-dissemination impacts, every property angle affects the transitions. Twofold diffusive convection of a micropolar liquid soaked in a permeable medium has numerous geotechnical applications, for example, underground atomic squanders, electro-synthetic procedures, contaminant transport in immersed soil, and drying forms.

The issue of twofold diffusive convection in a permeable medium immersed with Newtonian liquids has been broadly examined. Notwithstanding, consideration has not been given to the investigation of a twofold diffusive convection in a permeable medium layer soaked with a nanofluid. Notwithstanding, to the creators' best learning, very little consideration has been paid to the investigation of beginning of twofold diffusive convection of an inadequately pressed micropolar liquid in a permeable medium layer immersed by a nanofluid.

Subsequently, in this paper we think about the beginning of twofold diffusive convection of a micropolar liquid in a permeable medium layer soaked by a nanofluid. We examine the commitment of both Soret and Dufour impacts on the beginning of convection in nanofluids. The goal of this examination is to play out a direct soundness investigation with a typical mode system and nonlinear solidness investigation with a negligible portrayal of Fourier arrangement to figure warmth and mass vehicles qualities. Accentuation is put on how the beginning of convection is adjusted within the sight of nanoparticles. Additionally we research the impact of micropolar parameters on the beginning of convection.

2. Formulation of the problem and method of solution

We consider a micropolar liquid soaked permeable layer, kept between two vast flat surfaces, situated at $z^* = 0$ and $z^* = H$, warmed from beneath or above with a temperature distinction ΔT . The mass, force, inward rakish energy and vitality conditions, and nanoparticle conditions dependent on the Boussinesq estimate, together with the

Darcy-Brinkman-Forchheimer model for scantily pressed permeable liquid, are $\nabla^* \cdot \mathbf{v}_D^* = 0$,

(1)

$$\rho \left(\frac{D \mathbf{v}_D^*}{Dt} + \mathbf{v}_D^* \cdot \nabla^* \mathbf{v}_D^* \right) = -\nabla^* p + \nabla^* \cdot \boldsymbol{\tau} + \rho_0 \mathbf{g} + \mathbf{f} \quad (2)$$

$$\rho \left(\frac{D \boldsymbol{\omega}^*}{Dt} + \mathbf{v}_D^* \cdot \nabla^* \boldsymbol{\omega}^* \right) = \nabla^* \cdot \mathbf{c} + \mathbf{g} \quad (3)$$

$$\rho \left(\frac{D T^*}{Dt} + \mathbf{v}_D^* \cdot \nabla^* T^* \right) = \nabla^* \cdot \mathbf{q} + \dot{q} + \mathbf{v}_D^* \cdot \nabla^* p + \mathbf{v}_D^* \cdot \nabla^* \boldsymbol{\tau} + \mathbf{v}_D^* \cdot \nabla^* \boldsymbol{\omega}^* \quad (4)$$

$$\frac{D \phi^*}{Dt} + \mathbf{v}_D^* \cdot \nabla^* \phi^* = \nabla^* \cdot \mathbf{D}_B \nabla^* \phi^* + \nabla^* \cdot \mathbf{D}_T \nabla^* T^* + j \quad (5)$$

$$\frac{D p}{Dt} + \mathbf{v}_D^* \cdot \nabla^* p = \alpha' \nabla^* \cdot \boldsymbol{\tau} + \beta' \nabla^* \cdot \mathbf{c} + \gamma \nabla^* \cdot \mathbf{q} + K \nabla^* \cdot \boldsymbol{\omega}^* \quad (6)$$

where \mathbf{v}_D^* , $\boldsymbol{\omega}^*$ and T^* are respectively the velocity, the spin and the temperature. Here, $\mathbf{v}_D^* = (u^*, v^*, w^*)$ is the nanofluid Darcy velocity. Also, ρ is the total density, ρ_0 is the reference density, k_1 is the permeability, b is the Forchheimer constant, ϕ^* is the nanoparticle volume fraction, ε is the porosity, T^* is the temperature, D_B is the Brownian diffusion coefficient, and D_T is the thermophoretic diffusion coefficient. Further, p , μ , g and j are the thermodynamic pressure, the viscosity, the acceleration of gravity, and the microinertia constant. Here α', β', γ and K are the micropolar coefficients of viscosity. $(\rho c)_m$ and $(\rho c)_f$ are the heat capacity of the mixture and the fluid. k_m is the thermal conductivity and δ the coefficient representing the coupling between the spin and thermal effects.

The equation of state is given by

$$\rho = \rho_0 \left[1 + \beta_T (T^* - T_0) + \beta_C (C - C_0) \right] \quad (7)$$

where T_0 is the reference temperature at the lower boundary, C_0 is the reference solute concentration at the lower boundary, ρ_p is the particle density, β_T is the thermal expansion coefficient, and β_C is the analogous solutal expansion coefficient.

We assume that the temperature, solutal concentration, and the volumetric fraction of the nanoparticles are constant on the boundaries. Thus the appropriate boundary conditions are

$$\mathbf{v}_D^* = \mathbf{0} \quad \text{at } z^* = 0, \quad (8)$$

$$\mathbf{v}_D^* = \mathbf{0} \quad \text{at } z^* = H. \quad (9)$$

We introduce dimensionless variables as

$$\begin{aligned} & \nabla \cdot \mathbf{v} = 0, \\ & \rho \left(\frac{\partial \mathbf{v}}{\partial t} + \mathbf{v} \cdot \nabla \mathbf{v} \right) = -\nabla p + \mu \nabla^2 \mathbf{v} + \rho \mathbf{g} + \mathbf{F}, \\ & \rho \left(\frac{\partial \phi}{\partial t} + \mathbf{v} \cdot \nabla \phi \right) = D \nabla^2 \phi + \mathcal{L}(\phi, T, C), \end{aligned} \tag{10}$$

where

$$\frac{K_m}{\mu}, \frac{\rho_p}{\rho}$$

Then equations (1) - (9) take the form

$$\nabla \cdot \mathbf{v} = 0, \tag{11}$$

$$\begin{aligned} & \rho \left(\frac{\partial \mathbf{v}}{\partial t} + \mathbf{v} \cdot \nabla \mathbf{v} \right) = -\nabla p + \mu \nabla^2 \mathbf{v} + \rho \mathbf{g} + \mathbf{F}, \\ & \rho \left(\frac{\partial \phi}{\partial t} + \mathbf{v} \cdot \nabla \phi \right) = D \nabla^2 \phi + \mathcal{L}(\phi, T, C), \end{aligned} \tag{12}$$

$$\begin{aligned} & \rho \left(\frac{\partial \phi}{\partial t} + \mathbf{v} \cdot \nabla \phi \right) = D \nabla^2 \phi + \mathcal{L}(\phi, T, C), \\ & \rho \left(\frac{\partial T}{\partial t} + \mathbf{v} \cdot \nabla T \right) = \kappa \nabla^2 T + \mathcal{L}(T, \phi, C), \end{aligned} \tag{13}$$

$$\begin{aligned} & \rho \left(\frac{\partial \phi}{\partial t} + \mathbf{v} \cdot \nabla \phi \right) = D \nabla^2 \phi + \mathcal{L}(\phi, T, C), \\ & \rho \left(\frac{\partial C}{\partial t} + \mathbf{v} \cdot \nabla C \right) = D_C \nabla^2 C + \mathcal{L}(C, \phi, T), \end{aligned} \tag{14}$$

$$\begin{aligned} & \rho \left(\frac{\partial \phi}{\partial t} + \mathbf{v} \cdot \nabla \phi \right) = D \nabla^2 \phi + \mathcal{L}(\phi, T, C), \\ & \rho \left(\frac{\partial T}{\partial t} + \mathbf{v} \cdot \nabla T \right) = \kappa \nabla^2 T + \mathcal{L}(T, \phi, C), \end{aligned} \tag{15}$$

$$\begin{aligned} & \rho \left(\frac{\partial \phi}{\partial t} + \mathbf{v} \cdot \nabla \phi \right) = D \nabla^2 \phi + \mathcal{L}(\phi, T, C), \\ & \rho \left(\frac{\partial T}{\partial t} + \mathbf{v} \cdot \nabla T \right) = \kappa \nabla^2 T + \mathcal{L}(T, \phi, C), \end{aligned} \tag{16}$$

$$\begin{aligned} & \rho \left(\frac{\partial \phi}{\partial t} + \mathbf{v} \cdot \nabla \phi \right) = D \nabla^2 \phi + \mathcal{L}(\phi, T, C), \\ & \rho \left(\frac{\partial T}{\partial t} + \mathbf{v} \cdot \nabla T \right) = \kappa \nabla^2 T + \mathcal{L}(T, \phi, C), \end{aligned} \tag{17}$$

The parameter γ_a is the non-dimensional acceleration coefficient, Ln is a Lewis number, Va is a Vadász number, Pr is the Prandtl number, Da is the Darcy number, Ra_T is the thermal Rayleigh–Darcy number, and Rs is the solutal Rayleigh number. The new parameters Rm and Rn may be regarded as a basic-density Rayleigh number and a concentration Rayleigh number respectively. The parameter N_A is a modified diffusivity ratio and is somewhat similar to the Soret parameter that arises in cross-diffusion phenomena in solutions, while N_B is a modified particle-density increment. Interesting features of stationary or oscillatory convection depend on the choice of N_s . This will be discussed in a later section.

Equation (12) has been linearized by neglecting a term proportional to the product of ϕ and T . This assumption is likely to be valid in the case of small temperature gradients in a dilute suspension of nanoparticles.

2.2 Perturbation solution

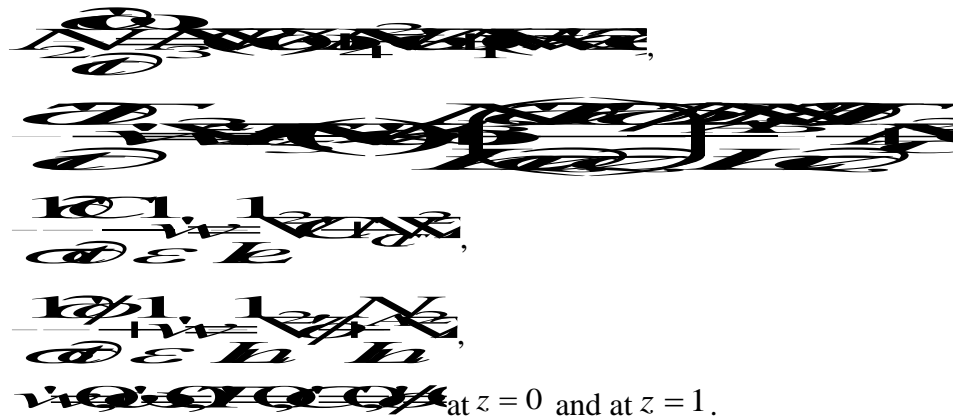
We now superimpose perturbations on the basic solution and write

$$\mathbf{v} = \mathbf{v}_0 + \mathbf{v}'$$

Substituting in equations (11) – (17) and linearizing (by neglecting products of primed quantities), we get the following equations:

$$\nabla \cdot \mathbf{v}' = 0,$$

$$\left(\gamma_a \frac{\partial \mathbf{v}'}{\partial t} + \nabla p' - Ra_T T' \hat{e}_z + Rn \phi' \hat{e}_z - \frac{Rs}{Le} C' \hat{e}_z \right) + \frac{(1+N_1)}{K} \mathbf{v}' - (1+N_1) \nabla^2 \mathbf{v}' - N_1 (\nabla \times \boldsymbol{\omega}') = 0,$$



Results and discussion

Figures 1a-f demonstrate the impact of different parameters on the impartial solidness bends for stationary convection with variety in one of these parameters. The impact of the Soret parameter and Dufour parameter on the warm Rayleigh number is appeared in Figs. 1a and 1b separately. It tends to be considered that to be and build, increments. Subsequently and advance the soundness of the framework. From Fig. 1c, one can see that as the solutal Rayleigh number R_s expands, the warm Rayleigh number abatements, which implies that the solutal Rayleigh number R_s propels the beginning of convection. The impact of micropolar parameters, and is appeared in Figs. 1d, 1e and 1f separately. Figs. 1d and 1f demonstrate that as and increment, builds, which shows that and will balance out the framework. The impact of the micropolar parameter on the warm Rayleigh number is appeared in Fig.1d. From this image, one can see that as increments, there is a reduction in the estimation of, consequently destabilizes the framework. The impact of the Soret parameter, Dufour parameter, and the solutal Rayleigh number R_s on warm Rayleigh number for stationary convection demonstrate the comparable outcomes to those acquired by Agarwal et al. [8].

Figures 2a-f show the variety of the warm Rayleigh number for oscillatory convection concerning different parameters. The impact of the Soret parameter and Dufour parameter on the warm Rayleigh number is appeared in Figs. 2a and 2b individually. It is considered that to be and expand, increments, and consequently and stabilizingly affect the framework. From Fig. 2c, one can see that as the solutal Rayleigh number R_s expands, the warm Rayleigh number abatements, which implies that the solutal Rayleigh number R_s progresses the beginning of convection. From the image 2d, one can see that the Vadász number V_a balances out the framework for oscillatory convection, that is, an expansion in V_a expands the warm Rayleigh number consequently postponing the beginning of convection. The impact of micropolar parameters on the warm Rayleigh number is appeared in Figs. 2e, 2g. It tends to be considered that to be the estimations of and increment, there is an expansion in the warm Rayleigh number, while in Fig. 2f, as the estimation of increments, there is a reduction in the warm Rayleigh number along these lines propelling the beginning of convection.

Subsequently it very well may be seen that the micropolar parameters and stabilizingly affect the beginning of convection for both stationary and oscillatory convection while the micropolar parameter destabilizes the framework.

Our nonlinear investigation gives not just the beginning edge of limited sufficiency movement yet in addition data about warmth and mass vehicle as far as the warm Nusselt number Nu_T , the nanoparticle focus Nusselt number Nu_F , and the solute fixation Nusselt number Nu_C . The Nusselt numbers are figured as elements of ν , and the varieties of these non-dimensional numbers with for various parameter esteems are delineated in Figs. 3a-e, 4a-e, and 5a-e separately. In Figs. 3a-e, 4a-e, and 5a-e, it is seen that for each situation, the nanoparticle focus Nusselt number Nu_F is constantly more noteworthy than both the warm Nusselt number Nu_T and the solute fixation Nusselt number Nu_C . All Nusselt numbers begin with the conduction state esteem 1 at the purpose of beginning of enduring limited sufficiency convection. At the point when ν is expanded past ν_c , there is a sharp increment in the estimations of the Nusselt numbers. Anyway further increment in ν won't change Nu and Sh essentially. It is to be noticed that the upper bound of Nu_T is 3. It ought to likewise be noticed that the upper bound of Nu_F and Nu_C are not 3. (Comparative outcomes were acquired by Bhadauria and Agarwal [9].) The upper bound of Nu_T remains 3 for both clear liquids and nanofluid. Then again, the upper headed for Nu_F and Nu_C for an unmistakable liquid is 3, yet for a nanofluid it isn't fixed.

From Figs. 3a and 4a, we see that as the Soret parameter builds, the estimation of Nu_T and Nu_F diminishes, along these lines demonstrating a decline in the rate of warmth and mass vehicle. Be that as it may, the Solute fixation Nusselt number Nu_C (Fig. 5a) increments with increment in Soret parameter inferring that the Soret parameter improves the Solute fixation Nusselt number. We see that as the Dufour parameter (Figs. 3b, 4b and 5b) and the solutal Rayleigh number Rs (Figs. 3c, 4c and 5c) increment, the estimation of Nu_T , Nu_F and Nu_C diminishes, consequently demonstrating an abatement in the rate of warmth and mass vehicle. As the micropolar parameter builds, the estimation of Nu_T increments while the estimations of Nu_F and Nu_C diminishes as can be found in Figs. 3d, 4d, and 5d separately. The impact of the porosity parameter on the beginning of convection is appeared in Figs. 3e, 4e and 5e. From every one of the plots one can see that as the estimation of increments, there is a reduction in the estimations of Nu_T , Nu_F , and Nu_C , hence demonstrating a diminishing in warmth and mass vehicle.

The straight arrangements show a significant assortment of practices of the framework, and the change from direct to non-direct convection can be very confounded. One must examination time-subordinate outcomes to break down this. The change can be surely known by the examination of condition (56) whose arrangement gives a point by point depiction of the two-dimensional issue. The self-sufficient arrangement of flimsy limited abundancy conditions is fathomed numerically utilizing the Runge-Kutta strategy. The Nusselt numbers are assessed as elements of time t . The flimsy transient conduct of Nu_T , Nu_F and Nu_C is appeared in Figs. 6a-I, 7a-I and 8a-I separately.

These figures show that at first, when time is little, there happen enormous scale motions in the estimations of Nusselt numbers demonstrating a precarious rate of warmth and mass vehicle in the liquid. Over the long haul, these qualities approach an unfaltering state comparing to a close convection arrange.

Figures (6a, 7a, 8a), (6b, 7b, 8b), (6c, 7c, 8c), and (6d, 7d, 8d) portray the transient idea of the warm Nusselt number Nu_T , the focus Nusselt number Nu_F , and the solute Nusselt number Nu_C on the nanoparticle fixation Rayleigh number Rn , nanofluid Lewis number Ln , adjusted diffusivity proportion ν , and the solutal Rayleigh number Rs . It is seen that as Rn , Ln , and Rs increment, Nu_T , Nu_F , and Nu_C increment, along these lines demonstrating an expansion in the warmth and mass vehicle. Comparable outcomes were seen by Agarwal et al. [8]. From Figs. (6f, 7f, 8f), (6g, 7g, 8g), (6h, 8h), and (6i, 7i, 8i), we see that in every one of these plots, the

micropolar parameters produce an expansion in the warmth and mass vehicle. From Fig. 7h, one sees that the micropolar parameter does not create much impact. In every one of these plots, it is fascinating to take note of that the impact of time on the transient warm Nusselt number Nu_T , the focus Nusselt number Nu_F , and the solute Nusselt number Nu_C is observed to be oscillatory when time is little. Notwithstanding, when time turns out to be extremely huge, all the Nusselt numbers, for example the warm Nusselt number Nu_T , the fixation Nusselt number Nu_F , and the solute Nusselt number Nu_C approach their consistent state esteems.

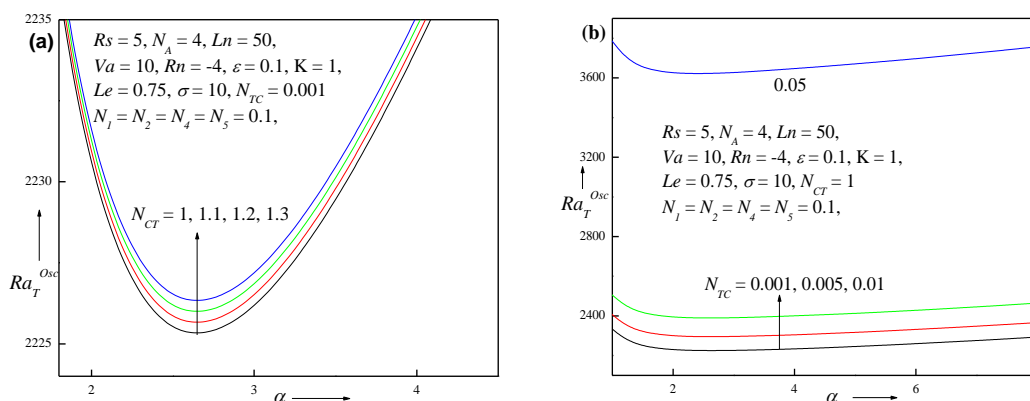
7. Conclusions

We summarize some of the interesting conclusions as follows.

1. and the micropolar parameters N_1, N_5 have a stabilizing effect while the solutal Rayleigh number Rs , the Vadász number Va , and the micropolar parameter N_4 destabilize the system.
2. The micropolar parameters relating to the thermal effects namely N_1, N_5 , have a stabilizing effect for both the stationary and oscillatory convections while the micropolar parameter N_4 destabilizes the system for both modes.

References

1. Lukaszewicz, G, Micropolar Fluids - Theory and Application, Birkhauser, Boston (1999).
2. Eringen, A.C., Theory of micropolar fluids, **16**, 1–18 (1966).
3. Lukaszewicz, G, Micropolar Fluids - Theory and Application, Birkhauser, Boston (1999).
4. Poulikakos, D., Double diffusive convection in a horizontal sparsely packed porous layer, Int. Comm. Heat Mass transfer **13**, 587-598 (1986).
5. Siddheshwar, P.G. and Pranesh, S., Magnetoconvection in a micropolar liquid, Int. J. Eng. Sci. **36**, 1173-1181 (1998).
6. Buongiorno, J., Convective transport in nanofluids, ASME J. Heat Transf. **128**, 240–250 (2006).
7. Nield, D.A., Onset of thermohaline convection in a porous medium, Water Resour. Res. **4**, 553–560 (1968).
8. Agarwal, S., Bhadauria, B.S., Sacheti, N.C., Chandran, P. and Singh, A.K., Non-linear Convective Transport in a Binary Nanofluid Saturated Porous Layer, Transp. Porous Media **93**, 29–49 (2012).
9. Bhadauria, B.S. and Agarwal, S., Natural convection in a nanofluid saturated rotating porous layer: A nonlinear study, Transp. Porous Media **87**, 585–602 (2011).



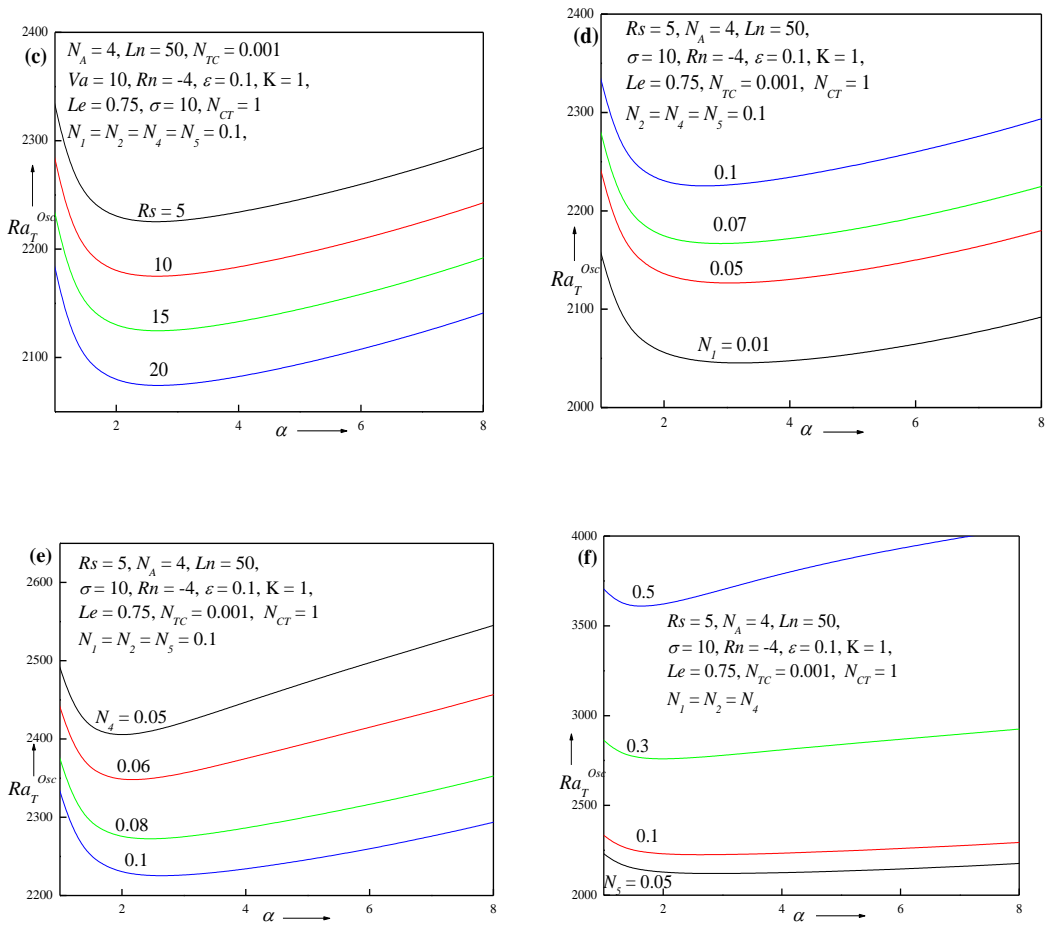
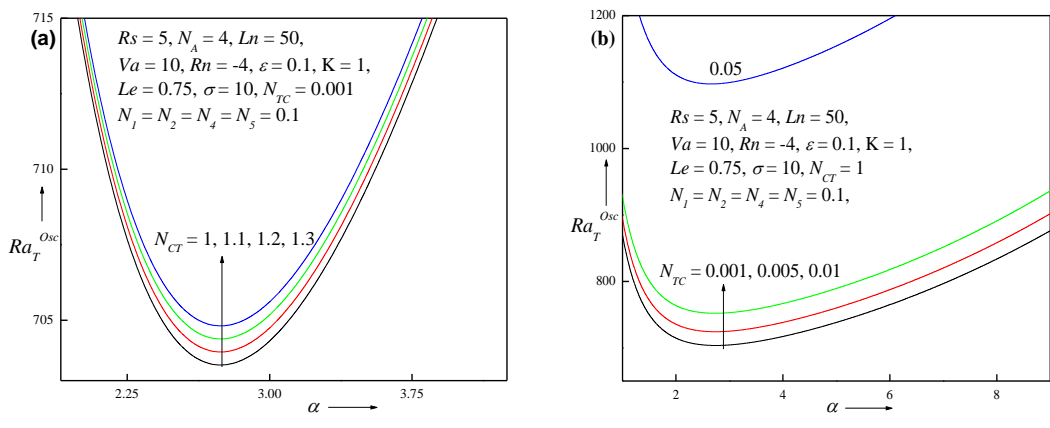


Fig. 1: Neutral stability curves of stationary convection for different values of
 (a) Soret parameter N_{CT} , (b) Dufour parameter N_{TC} , (c) solutal Rayleigh number Rs , (d) micropolar parameter N_1 , (e) micropolar parameter N_4 , (f) micropolar parameter N_5 .



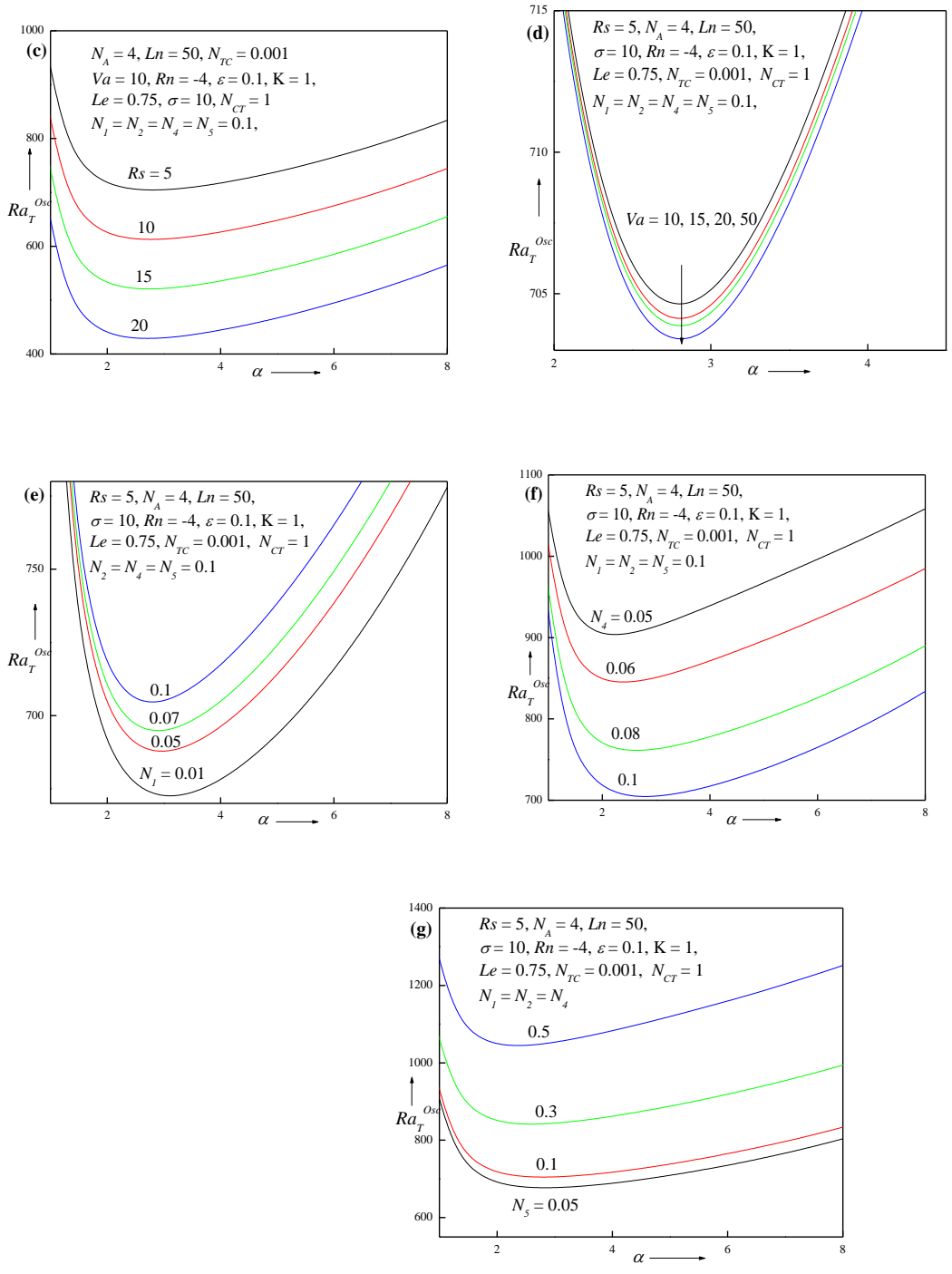


Fig. 2: Neutral curves on oscillatory convection for different values of
 (a) Soret parameter N_{CT} , (b) Dufour parameter N_{TC} , (c) solutal Rayleigh number Rs , (d) Vadász number Va , (e) micropolar parameter N_1 , (f) micropolar parameter N_2 , (g) micropolar parameter N_4 .

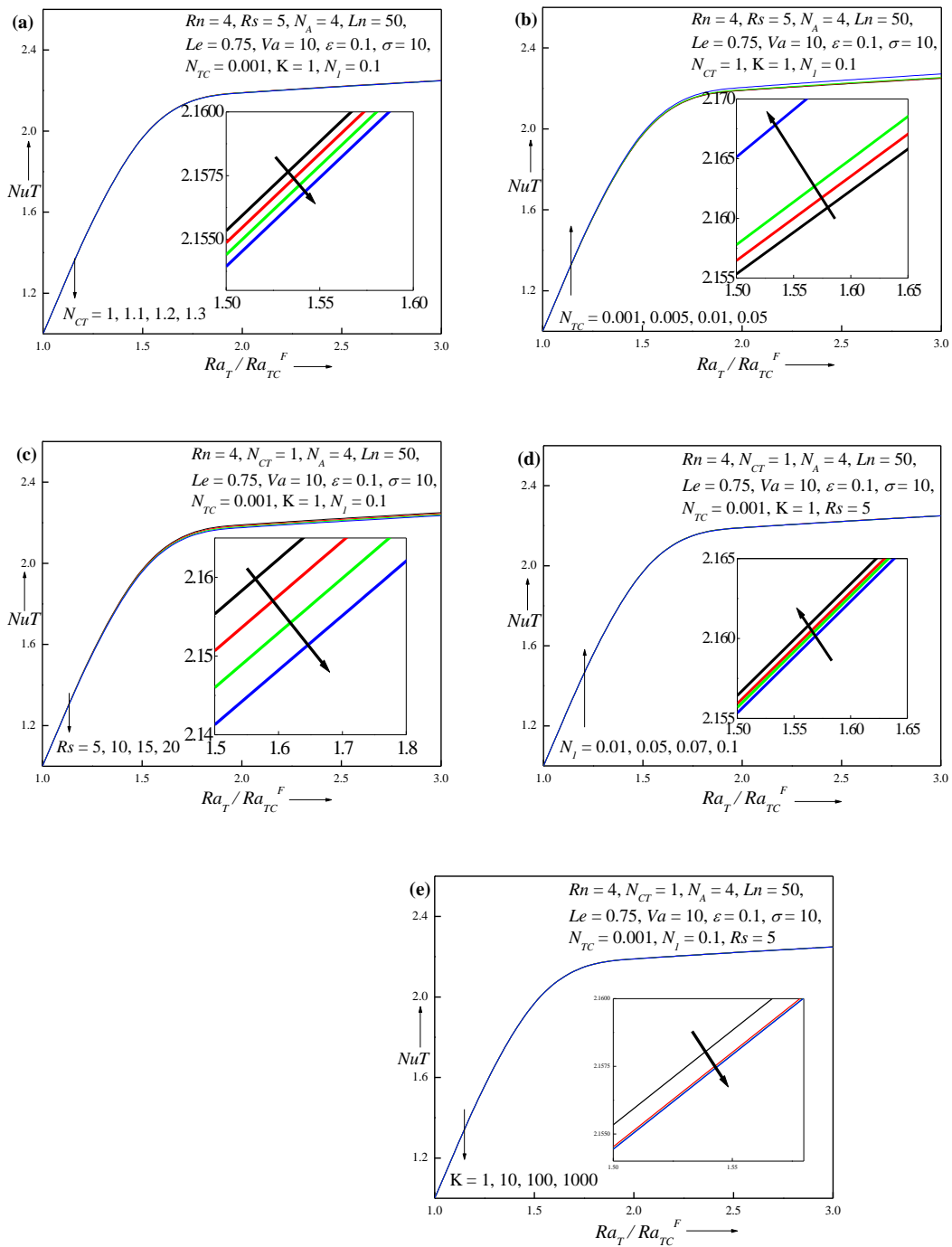


Fig. 3: Variation of thermal Nusselt number NuT with critical Rayleigh number for different values of (a) Soret parameter N_{CT} , (b) Dufour parameter N_{TC} , (c) solutal Rayleigh number Rs , (d) micropolar parameter N_i , (e) porous parameter K .

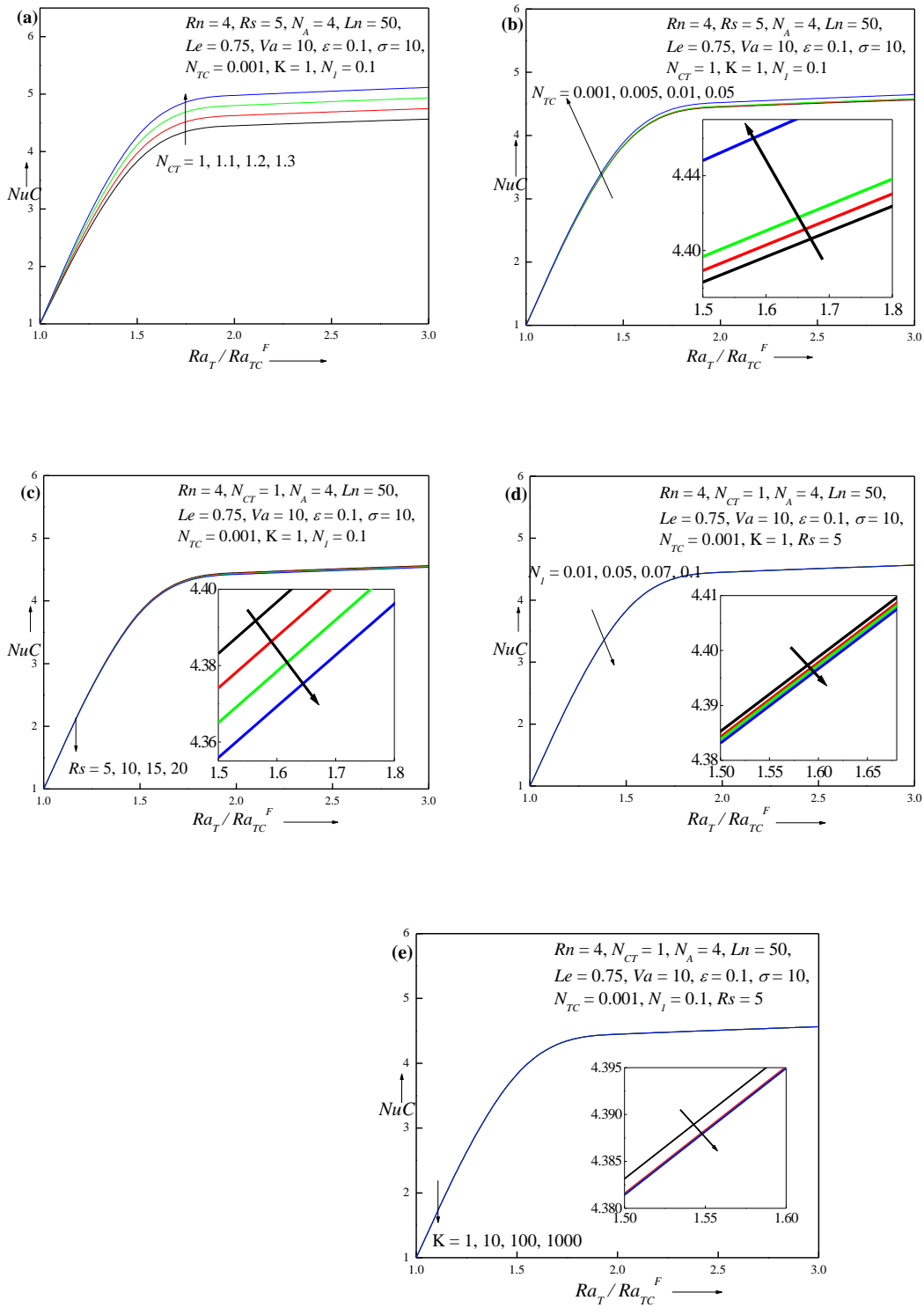


Fig. 4: Variation of solute concentration Nusselt number Nu_C with critical Rayleigh Number for different values of (a) Soret parameter N_{CT} , (b) Dufour parameter N_{TC} , (c) solutal Rayleigh number Rs , (d) micropolar parameter N_I , (e) porous parameter K .

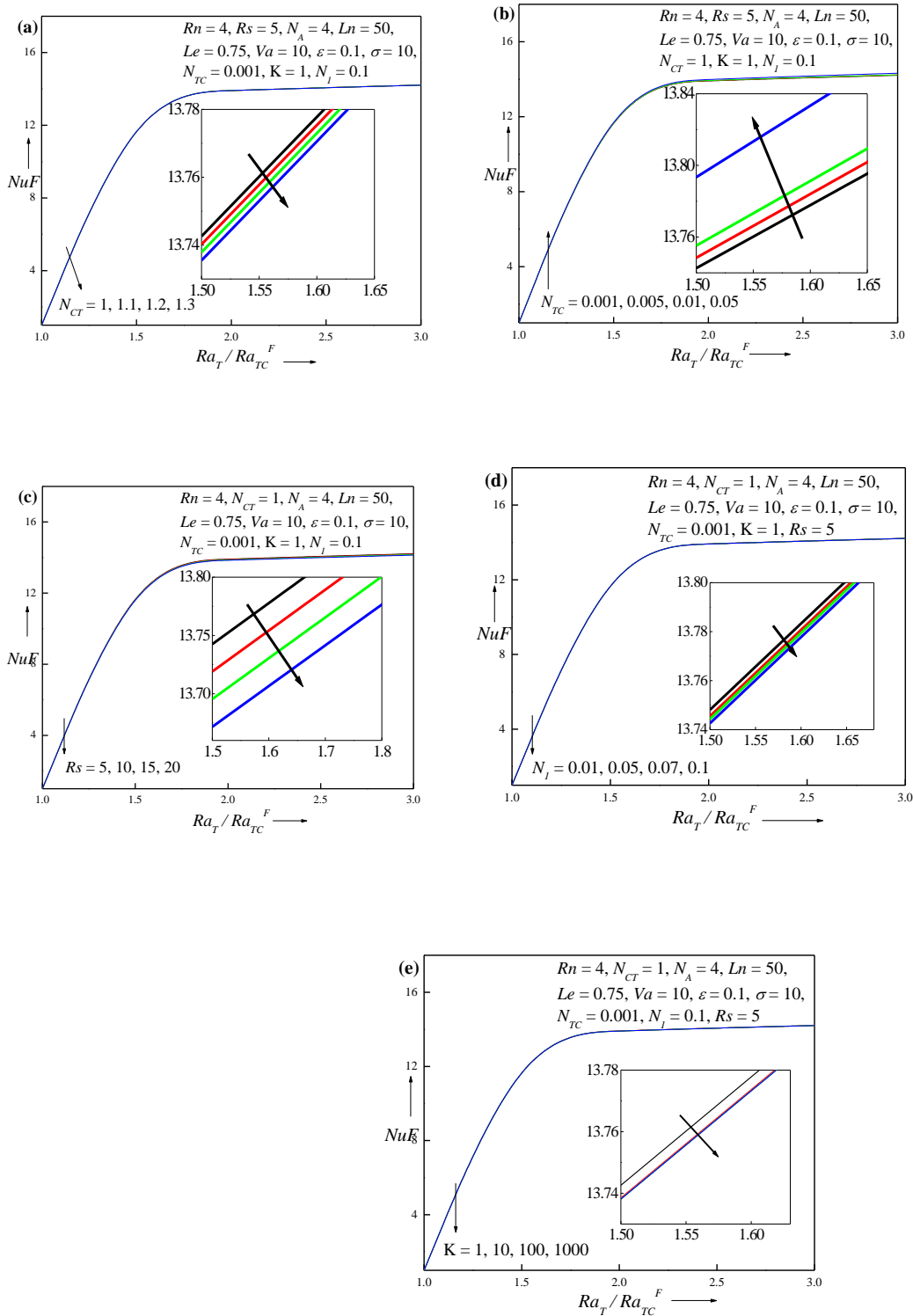
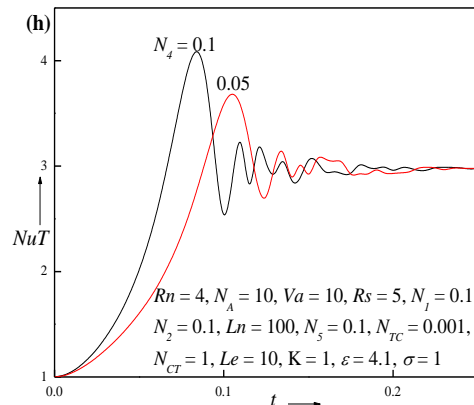
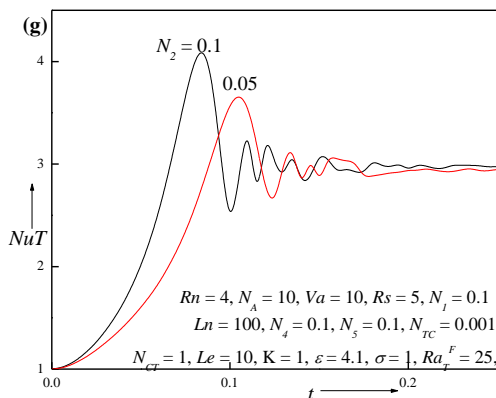
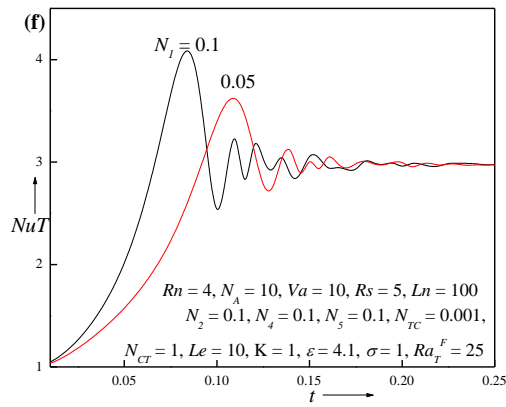
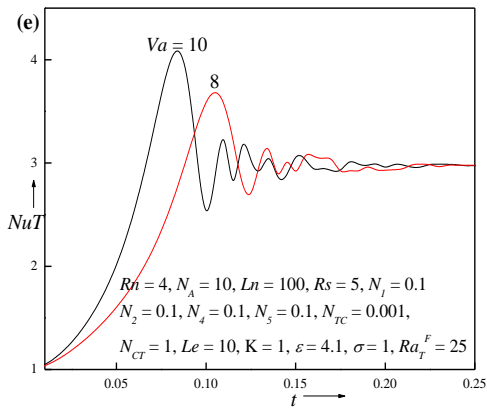
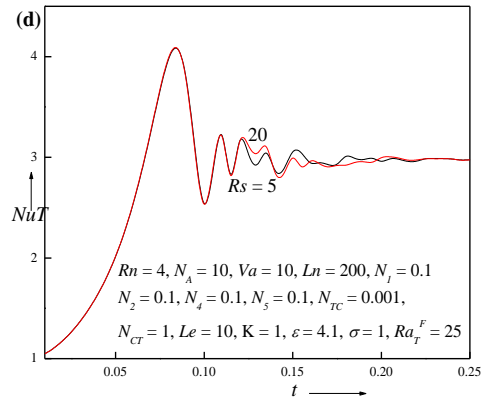
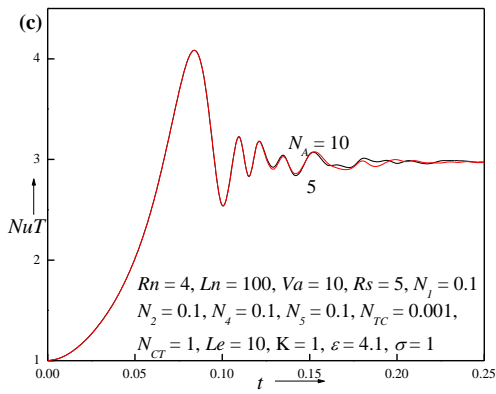
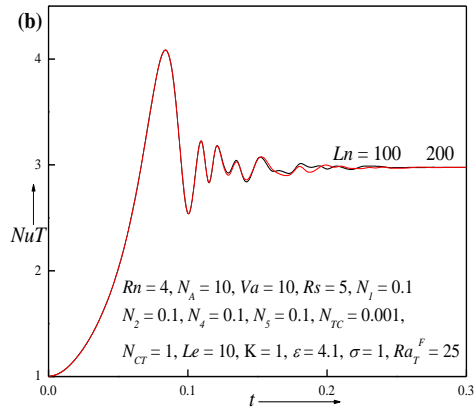
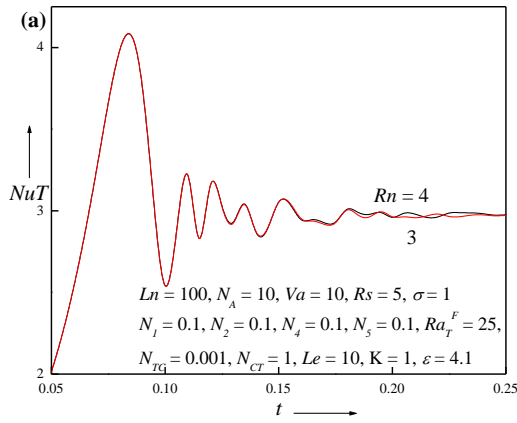


Fig. 5: Variation of nanoparticle concentration Nusselt number NuF with critical Rayleigh number for different values of (a) Soret parameter N_{CT} , (b) Dufour parameter N_{TC} , (c) solutal Rayleigh number Rs , (d) micropolar parameter N_1 , (e) porous parameter K .



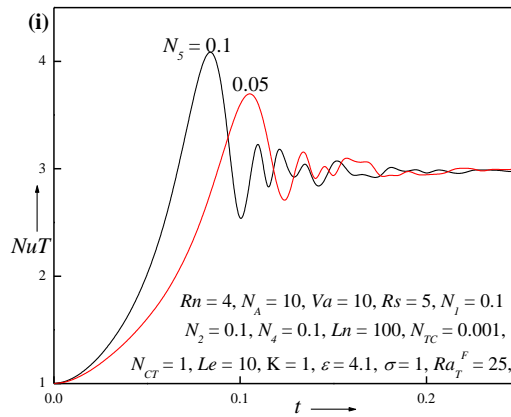
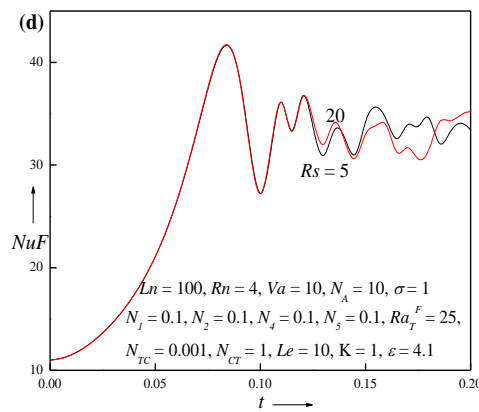
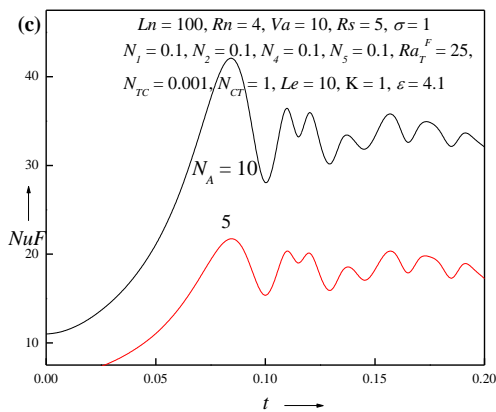
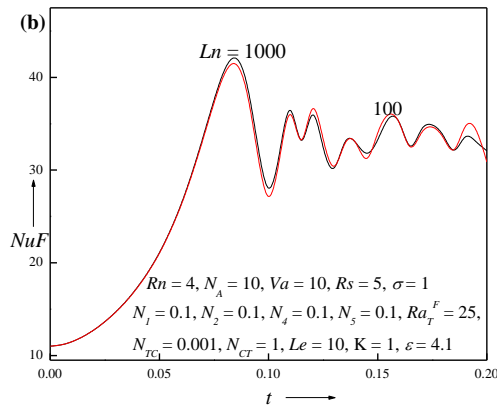
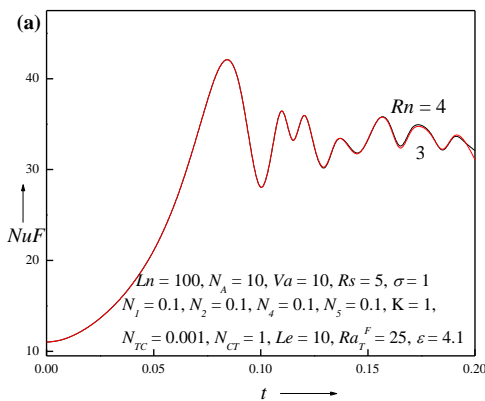


Fig. 6: Transient thermal Nusselt number NuT with time for different values of
 (a) Nanoparticle concentration Rayleigh number Rn , (b) thermo-nanofluid Lewis number Ln , (c) modified diffusivity ratio N_A , (d) solutal Rayleigh number Rs , (e) Vadász number Va , (f) micropolar parameter N_1 , (g) micropolar parameter N_2 , (h) micropolar parameter N_4 , (i) micropolar parameter N_5 .



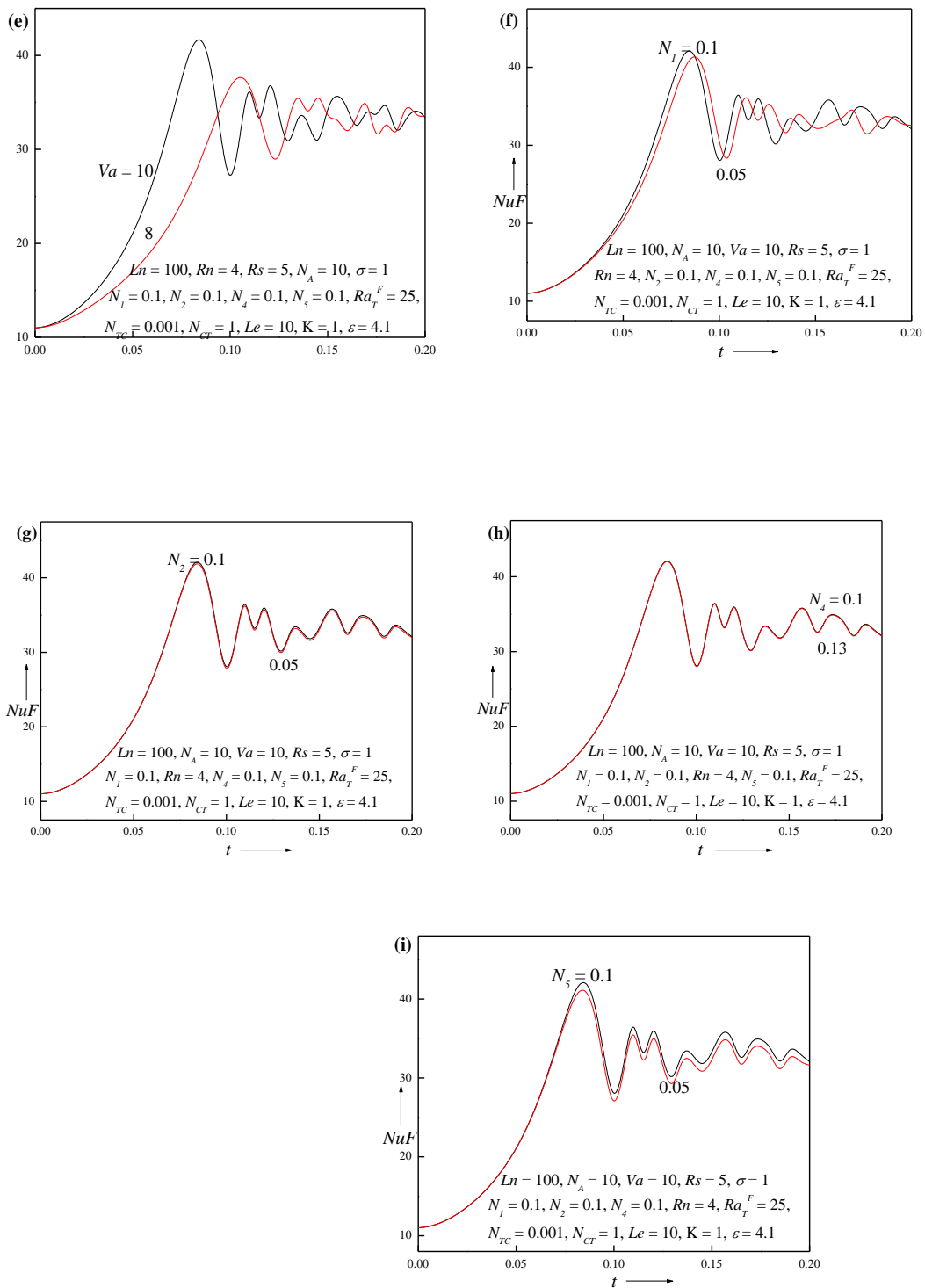
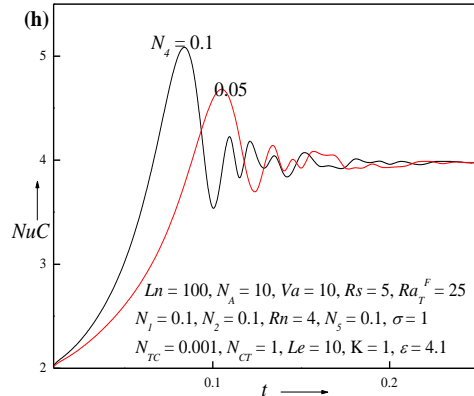
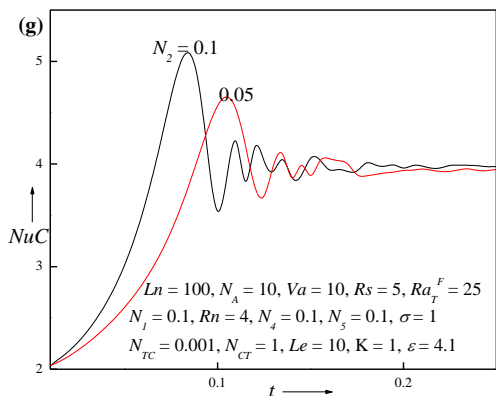
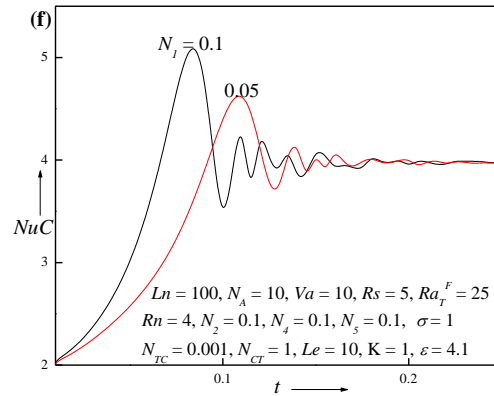
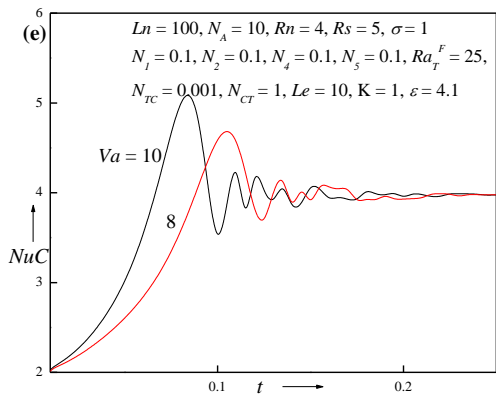
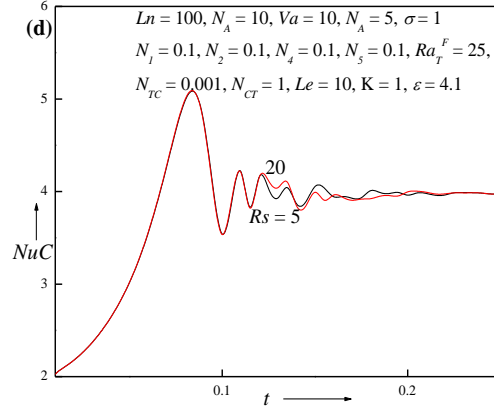
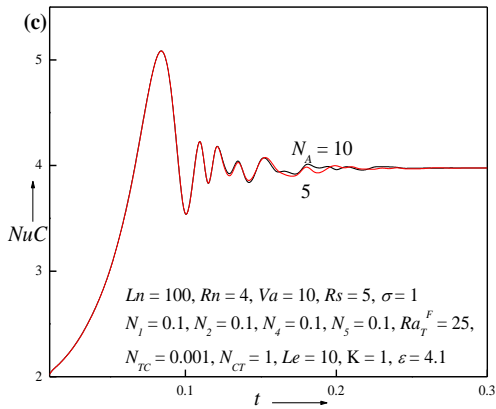
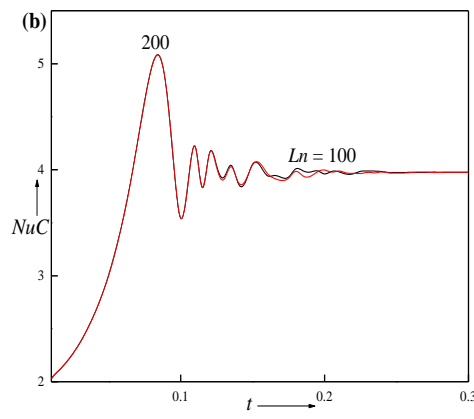
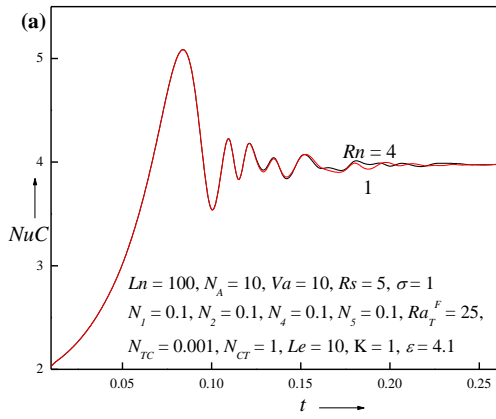


Fig. 7: Transient nanoparticle concentration Nusselt number NuF with time for different values of (a) nanoparticle concentration Rayleigh number Rn , (b) thermo-nanofluid Lewis number Ln , (c) modified diffusivity ratio N_A , (d) solutal Rayleigh number Rs , (e) Vadász number Va , (f) micropolar parameter N_1 , (g) micropolar parameter N_2 , (h) micropolar parameter N_4 , (i) micropolar parameter N_5 .



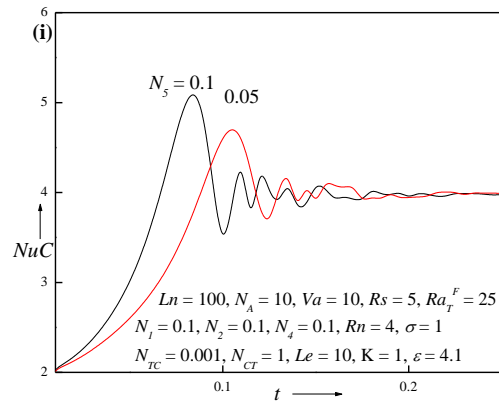


Fig. 8: Transient solute concentration Nusselt number NuC with time for different values of (a) nanoparticle concentration Rayleigh number Rn , (b) thermo-nanofluid Lewis number Ln , (c) modified diffusivity ratio N_A , (d) solutal Rayleigh number Rs , (e) Vadász number Va , (f) micropolar parameter N_1 , (g) micropolar parameter N_2 , (h) micropolar parameter N_4 , (i) micropolar parameter N_5 .